This is the author's version of the article that has been published at the Proc. Int. Conf. Unmanned Aircraft Syst., Atlanta, GA, USA, 2019, pp. 628-635.

# Multi-UAV based Autonomous Wilderness Search and Rescue using Target Iso-Probability Curves

Zendai Kashino, *Student Member, IEEE*, Goldie Nejat, *Member, IEEE*, Beno Benhabib
*Department of Mechanical and Industrial Engineering, University of Toronto*
Toronto, Canada
zendkash@mie.utoronto.ca, nejat@mie.utoronto.ca, benhabib@mie.utoronto.ca

***Abstract*—The application of unmanned aerial vehicles (UAVs) to searches of lost persons in the wilderness can significantly contribute to the success of the missions. Maximizing the effectiveness of an autonomous multi-UAV search team, however, requires optimal task allocation between the team members, as well as the planning of the individual flight trajectories. This paper addresses this constrained resource-allocation optimization problem via the use of iso-probability curves that represent probabilistic target-location information in a search region growing with time. The optimization metric used is the allocation of the search effort proportional to the target location likelihood. The proposed method also avoids redundancy in coverage while planning the UAV trajectories.**

**Numerous simulated search experiments, two of which are detail herein, were carried out to demonstrate our method's effectiveness in wilderness search and rescue (WiSAR) planning using a multi-UAV team. Extensive comparative studies were also conducted to validate the tangible superiority of our proposed method when compared to existing WiSAR techniques in the literature.**

***Keywords—Autonomous mobile-target search, multi-UAV task allocation, iso-probability curves, wilderness search and rescue*[1]**

## I. Introduction

Unmanned aerial vehicles (UAVs) can be used for a wide range of applications, including archaeology [1]–[3], environmental monitoring [4]–[6], agriculture [7]–[9], structural health monitoring [10]–[12], surveillance [13]–[15], and search and rescue [16]–[19]. Wilderness search and rescue (WiSAR) is of particular interest for UAVs, however, as it poses many challenges in terms of target detection, target motion prediction, and search planning.

In general, research into UAV use in search and rescue has been primarily focused on target-detection methods [20]–[22], system design and evaluation [23]–[26], and search path/trajectory planning [27]–[37]. Target-detection methods are concerned with how to recognize targets once they are in the field of view of the UAV. For example, in [20], a method of detecting the target in images acquired from a UAV using two *k*-means classifiers was discussed.

System design and evaluation literature is, typically, concerned with how UAV systems are used to perform WiSAR. For example, in [23], the performance of a UAV-based WiSAR support system was examined in a field experiment simulating a real-world search scenario. The study identified several issues that need to be resolved in order to improve search performance, including the high computational demand of analyzing data acquired from the UAVs and the high bandwidth demand for transferring UAV acquired data to a remote processing location.

Since, in the WiSAR problem, the exact location of the target is unknown for the entirety of the search, most methods make use of a probabilistic model to represent possible target locations [27]–[30]. A UAV trajectory is, then, planned to maximize the probability of target detection given this model. For example, in [27], UAV search utilized a target location likelihood function defined over the search area. The likelihood function was modified in a Bayesian manner based on latest UAV observations. Other works aim to achieve coverage or detection guarantees through a specifically designed trajectory. For example, the work in [31] proposed an outward spiral trajectory that guaranteed the target was not within areas already searched by the UAV. In [32], an inward spiral trajectory is proposed which guarantees target detection within a bounded area. Others combine coverage and probabilistic path planning, in order to examine a set of high-probability areas as efficiently as possible. For example in [33], the problem of visiting and covering a set of disjoint search areas was formulated as a combined traveling-sales-person and coverage-path planning problem.

Similar work has been carried out regarding search planning using unmanned ground vehicles (UGVs) and wireless sensor networks (WSNs). For example, in [38], UGV paths were planned to search for a lost person and made use of a novel target location likelihood representation [39]. The work in [40], [41] presented a method for planning a time-phased WSN for maximizing target detection in mobile-target search. The work was extended in [42], [43] by additionally planning UGV delivery of sensors according to the optimal sensor-network deployment plan.

In this paper, we propose a new multi-UAV motion planning method for WiSAR. The method's novelty includes optimal task allocation as well as trajectory planning via the extension of the use of iso-probability curves into the

[1] This research was funded in part by the Natural Sciences and Engineering Research Council of Canada (NSERC), and the Canada Research Chairs program.

continuous domain, where the UAVs traverse a range of iso-probability curves throughout the search. The proposed method also considers pseudo-redundant coverage, a dynamic analog of redundant coverage, to improve search effectiveness.

In Section II we begin describing our method by first outlining the assumptions made in the search scenario considered and some background on iso-probability curves and pseudo-redundant coverage. Then, the planning problem being addressed is formalized in Section III. The method of UAV trajectory planning is described in Section IV and is followed by illustrative simulated experiments in Section V.

## II. Assumptions and Background

### A. Assumptions

In WiSAR, information known at the start of the search is, typically, limited to the lost person's (target's) demographic, his/her last known position (LKP), search-area terrain, and search-resources availability. Commonly, a (statistical) target mobility model can be generated based on this information. In such a model, the target would be assumed to wander randomly by, for example, moving along a fixed heading for a random distance before randomly changing directions [40].

Two parameters define the characteristics of the target's motion in the model used in this work: $\sigma_\theta$ and $d_{\max}$. The former specifies the degree of wandering. Namely, it is the standard deviation of the headings chosen by the target. The latter characterizes the target's indecisiveness. Namely, it represents the maximum distance the target would continue traveling along a given heading. Since the model assumes that the target is always mobile, the search area (the region wherein the target could be) increases in size over time.

Several assumptions need to also be made regarding the search agents' capabilities (UAVs in our case). First, it is assumed that all UAVs have global positioning and communication capabilities. Furthermore, a binary disk model of detection is assumed. Namely, if the target passes within the sensing radius of any UAV, it is assumed to have been detected.

### B. Background

The UAV search-planning method proposed herein utilizes the concept of iso-probability curves to represent probabilistic target-location information, first presented by our group in [39]. It also uses the concept of pseudo-redundant coverage to increase the effectiveness of search planning [31].

#### 1) Iso-Probability Curves

Iso-probability curves encircle the target's LKP and denote the farthest that the slowest $P^{\text{th}}$ percentile target could reach after a given amount of time in any given direction [39]. Since the target is assumed to be dynamic, these curves grow with time. Fig. 1 shows an example set of iso-probability curves for a target with an assumed normally-distributed outward propagation rate, at times $t$ and $t + \Delta t$. The red, green, and blue curves represent the 30%, 50%, and 70% curves, respectively. The non-uniformity of the curves is due to terrain variability.

In this paper, iso-probability curves are used to guide search planning. Namely, UAVs are assigned to track a set of iso-probability curves for the duration of the search. The range of curves assigned to each UAV, individually, need to be optimally selected to maximize the probability of successful target detection.

#### 2) Pseudo-Redundant Coverage

One of our goals, herein, is also to avoid redundant coverage, in order to increase the effectiveness of the search. Redundant coverage is, typically, defined as revisiting an area that has already been searched. However, since in WiSAR, the target is often assumed to be mobile, repeated coverage of the same area is not always detrimental. Namely, the target can move back into an already searched area. Thus, true redundant coverage does not exist in a dynamic search problem. Instead, *pseudo-redundant coverage* is considered.

In the above context, the *confidence area* was defined in [31] as one that we are confident the target is not located within. For example, let us consider a sensor, with a detection radius of $r_s$, that can be *polled* to determine whether the target is within it. However, even if the target were not within the detection area initially, as time passes, this area would shrink in size due to the probability of the target revisiting the region. Psuedo-redundant coverage, then, occurs when a searcher revisits part of the confidence area.

Fig. 2 shows the confidence area around a UAV spiral trajectory. The area is a continuous collection of the confidence area circles around positions the UAV has passed at discrete times. In the figure, the UAV is, currently, at the $t_5$ position, where $t_0 < t_1 < t_2 < t_3 < t_4 < t_5$. One may note that all past circles have progressively diminished from their original size (with a detection radius of $r_s$) shown at $t_5$. Namely, as the UAV travels forward along its trajectory, the confidence circles around past locations shrink. The speed at which the overall confidence area shrinks is equal to the maximum speed at which the target can move.

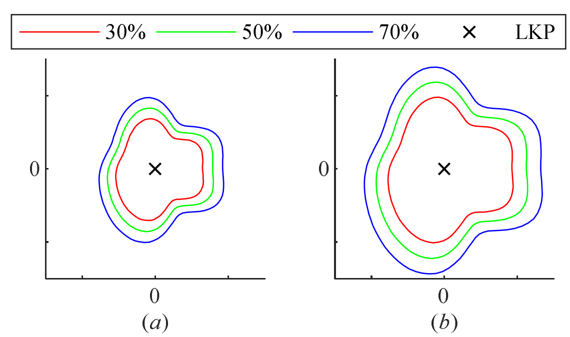


Fig. 1. An example set of iso-probability curves at (*a*) $t$, and (*b*) $t + \Delta t$.

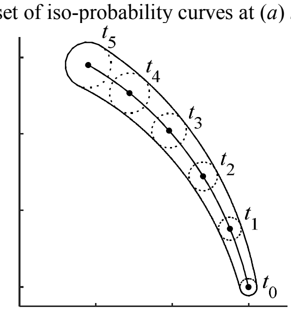


Fig. 2. The confidence area around a UAV path.

This is the author's version of the article that has been published at the Proc. Int. Conf. Unmanned Aircraft Syst., Atlanta, GA, USA, 2019, pp. 628-635.

## III. Problem Formulation

The specific problem we address is to plan UAV search trajectories that maximize the probability of target detection. This is a constrained resource-allocation optimization problem. It is assumed the search effort should be allocated proportional to the target location likelihood. This conjecture is based on the definition of the probability of successful target detection (POS). Namely, POS is a product of the probability of the target being in the area (POA) and the probability of detecting the target (POD), if it is in the area [44]:

$$\text{POS} = \text{POA} \times \text{POD}. \tag{1}$$

Above, the total probability of successful target detection is, then, the sum of POS over all locations in the search area.

If POD were proportional to the search effort expended at a location, the problem of maximizing the total POS would have a *greedy* solution. Namely, exhaustively searching locations with high POA before moving onto locations with lower POA. However, in a dynamic problem, there exist diminishing returns to spending more search effort at a given location. Namely, POD increases sub-linearly with the amount of search effort expended at a location. As such, it would be beneficial to diversify by searching a variety of possible target locations instead of exhaustively searching where the target is most likely to be found.

A balance between exploiting locations with high POA and exploring a range of locations can be struck by allocating search effort in a way that is proportional to the POA. Thus, the problem addressed herein is one of planning a search which distributes search effort proportionally to the target location likelihood.

## IV. Proposed UAV Search Planning Method

The proposed UAV search planning method is based on the optimal search of a range of iso-probability curves. Namely, the UAVs traverse across iso-probability curves continuously throughout the search, as opposed to remaining on any given one curve as time progresses.

### A. Single-UAV Search Planning

As noted above, in Section III, an optimal search for a dynamic problem is one in which the search effort is distributed over the search area proportionally to the target location likelihood. Iso-probability curves, by definition, employ such proportionality. Thus, an optimal way to distribute search effort on iso-probability curves would be to spend an equal amount of search effort on all curves.

#### 1) Equal-Effort Search

Let us consider, first, the discrete case where there exists a finite set of equally spaced (in terms of percentile) iso-probability curves to search. Optimal search by a single UAV could be achieved by having the UAV switch between these curves while spending an equal amount of search effort on each one. Herein, we extend this idea to the continuous domain. Namely, the equivalent of spending continuously an equal amount of search effort on discrete curves is traversing a continuum of curves at a constant rate with respect to search effort expended. Thus, we propose to plan UAV motion such that the UAV traverses iso-probability curves at an equal rate with respect to search effort expended.

Let $p(E(t))$ denote the percentile iso-probability curve upon which the UAV is on after expending a time-cumulative search effort $E(t)$. UAV motion can, then, be planned such that the change in target percentile being searched, $dp(E(t))$, is proportional to the change in effort expended, $dE(t)$:

$$dp(E(t)) = C dE(t), \tag{2}$$

where $C$ is the constant rate of curve progression with respect to search effort expended.

In order to consider all possible target motions, the UAV must start on the 0% iso-probability curve and end on the 100% curve. Integrating (2) with these boundary conditions, an explicit expression of $p(E(t))$ can be determined:

$$p(E(t)) = CE(t), \tag{3}$$

where

$$E(t_{start}) = 0 \text{ and } E(t_{end}) = 1/C. \tag{4}$$

Above, $t_{start}$ is the start time of the search and $t_{end}$ is the end time.

Effort expended searching for the target can be expressed in terms of the proportion of possible target propagation directions the UAV searches. Thus, the cumulative effort expended, $E(t)$, can be expressed as being proportional to the cumulative angular motion of the UAV. However, if it is assumed that the UAV's angular position increases monotonically (i.e., it only moves clockwise) as in [38], this can be further simplified. Namely, the cumulative effort expended can be expressed as being proportional to the angular position of the UAV:

$$E(t) \propto \theta(t), \tag{5}$$

where $\theta(t)$ is the UAV's angular position over time.

Since any constant factor differentiating $E(t)$ from $\theta(t)$ can be absorbed into $C$, we can define a new constant $C'$ and determine an explicit equation for $p(\theta(t))$ as a function of $\theta(t)$:

$$p(\theta(t)) = C'\theta(t). \tag{6}$$

Thus, for an optimal search, a UAV is required to traverse the iso-probability curves at a constant rate with respect to its angular position.

##### a) The Static Iso-probability Curve Case

For simplicity, let us first consider the static iso-probability curve case, where it remains frozen in its position at some time $t_0$. In this case, the radial position of the UAV is given by:

$$r(\theta) = r_{p(\theta)}(\theta, t_0), \tag{7}$$

where $r_{p(\theta)}(\theta, t_0)$ is the intersection point between the $p(\theta)$% iso-probability curve at time $t_0$ and a ray in direction $\theta$. The optimal search path in polar coordinates is, then:

$$\boldsymbol{x}_u(\theta) = (\theta, r(\theta)). \tag{8}$$

Namely, the UAV search path is expressed independently of time. A trajectory can, then, be defined by assuming the UAV traverses this path as fast as possible.

Eq. (8) is a description of the path traversed by the UAV, given $p(\theta)$. The rate of curve progression, $C$, used in $p(\theta)$ must be optimized such that the UAV arrives at the 100% iso-probability curve at $t_{end}$ (i.e., to satisfy (4)). Qualitatively, $C$ influences how tightly wound the UAV search trajectory is. A lower $C$ results in a more tightly wound and thorough search and, thus, a later arrival by the UAV at the 100% iso-probability curve. The opposite is true for higher $C$ values. Optimization methods such as gradient descent or Newton's method could be used to obtain the optimal $C$ value.

An example search path and a plot of the UAV's radial position over time are shown in Fig. 3.

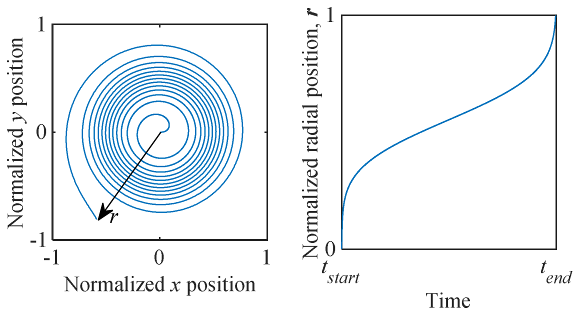


Fig. 3. An example UAV search trajectory for the static case.

### b) The Dynamic Iso-probability Curve Case

The actual UAV search-planning problem is more complex since the iso-probability curves are dynamic. Namely, the UAV is required to traverse iso-probability curves that are propagating outward away from the LKP. In order to formulate this problem, let us first consider a general description of the path the UAV would need to follow. Since the iso-probability curve positions vary with time, the desired radial position of a UAV is also time dependent. Namely it is a function of the UAV's time-dependent angular position, $\theta(t)$, as well as the time at which it is at that angular position:

$$r(t) = r_{p(\theta(t))}(\theta(t), t). \tag{9}$$

The overall trajectory in polar coordinates can, thus, be described as:

$$\boldsymbol{x}_u(t) = (\theta(t), r_{p(\theta(t))}(\theta(t), t)). \tag{10}$$

Due to UAV velocity constraints, the UAV trajectory additionally needs to be planned such that it always moves at its maximum velocity:

$$\|d\boldsymbol{x}_u(t)/dt\| = v_u, \tag{11}$$

where $\|\cdot\|$ is the Cartesian norm.

The search planning problem is, then, one of determining a trajectory wherein in the UAV traverses across iso-probability curves in the prescribed manner, (10), while always moving at its maximum velocity, (11). For simplicity, let us consider the discrete case, in which the UAV switches between discrete iso-probability curves. This converts the trajectory-following problem into a series of interception problems.

The interception problem at hand is one of planning UAV motion to intercept the next iso-probability curve after expending some amount of search effort on the current curve. Since search effort expended is proportional to the amount of angular motion, this equates to intercepting the next (moving) iso-probability curve after moving a fixed amount in the angular direction. Namely, the problem can also be expressed as one of planning UAV motion to intercept a point defined by the intersection of the next iso-probability curve and a ray extending from the LKP.

Let us examine the scenario presented in Fig. 4, where a UAV is required to move from its current position on the $p(\theta_1)$% iso-probability curve (blue dashed line), at $\boldsymbol{x}_{u1} = (\theta_1, r_{p(\theta_1)}(\theta_1, t_1))$ (black circle), to a position on the next iso-probability curve, the $p(\theta_2)$% iso-probability curve (red dotted line), at $\boldsymbol{x}_{u2} = (\theta_2, r_{p(\theta_2)}(\theta_2, t_2))$ (black square). In this case, the interception problem is one of planning UAV motion to reach the destination, $\boldsymbol{x}_{u2}$, as it moves radially outwards along the $\theta_2$ ray with the starting point $\boldsymbol{x}_{u1}$.

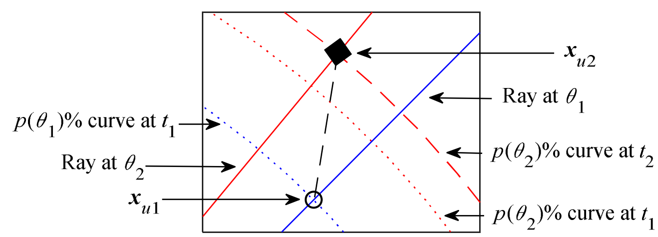


Fig. 4. The interception problem in the dynamic curve case.

Let us suppose that $\boldsymbol{x}_{u2}$ is propagating radially outwards along the $\theta_2$ ray with a speed of $v_2$ at time $t_1$. The position of $\boldsymbol{x}_{u2}$ at a later time, $t_2$, can, then, be approximated as:

$$\boldsymbol{x}_{u2}(t_2) = \boldsymbol{x}_{u2}(t_1) + v_2\,(t_2 - t_1)\,(\cos(\theta_2), \sin(\theta_2)). \tag{12}$$

Assuming that the UAV will move in a straight line with speed $v_u$ from $\boldsymbol{x}_{u1}$ to intercept $\boldsymbol{x}_{u2}$, we need:

$$|\,\boldsymbol{x}_{u2}(t_2) - \boldsymbol{x}_{u1}\,| = v_u\,(t_2 - t_1), \tag{13}$$

where $|\cdot|$ is the Cartesian norm. Since this is quadratic in $t_2$, it is possible to solve for the interception time and, therefore, the interception location. Once it is known when the UAV will be at $\boldsymbol{x}_{u2}$, the process can be repeated for the UAV traversing between $\boldsymbol{x}_{u2}$ and $\boldsymbol{x}_{u3}$, and, then, for $\boldsymbol{x}_{u3}$ and $\boldsymbol{x}_{u4}$, etc., until the end of the search time is reached.

One can note that, as in the static case, the rate of curve progression $C$ needs to be optimized, such that the UAV arrives at the 100% iso-probability curve at $t_{end}$.

Fig. 5 shows an example search trajectory and a plot of the UAV's radial position over time in the dynamic case.

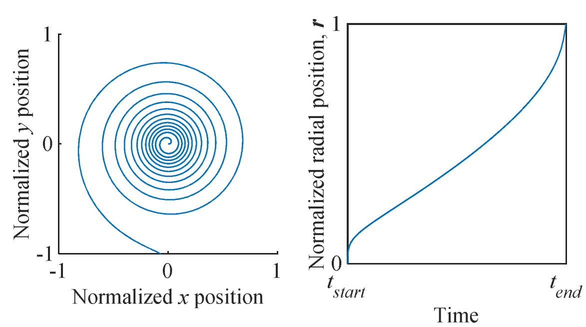


Fig. 5. An example UAV search trajectory for the dynamic case.

*2) Pseudo-Redundant Coverage*

In addition to following an optimal search trajectory, UAV motion must be planned to minimize redundancy in coverage. In our case, pseudo-redundant coverage would occur when a UAV goes around, on an iso-probability curve, and revisits areas still in the *confidence area*. Such coverage can be avoided by shifting the UAV's trajectory.

*a) The Static Iso-probability Curve Case*

For simplicity, let us first consider the static iso-probability curve case, where it remains frozen in its position at some time $t_0$. In this case, an iso-probability curve of length $l$ is searched by a UAV with speed $v_u$ and a detection radius of $r_u$. Given a maximum target speed of $v_{t\max}$, pseudo-redundant coverage would occur if, after the UAV makes one round of the curve, the *confidence area* has not disappeared at the UAV's original location, Fig. 2.

Since the confidence area at the UAV's initial location starts as a circle of radius $r_u$ and diminishes at a rate of $v_{t\max}$, pseudo-redundant coverage would occur if the time it takes for the UAV to make one round of the iso-probability curve is less than the time it takes for the confidence area to disappear:

$$l/v_u < r_u/v_{t\max}. \tag{14}$$

Given that pseudo-redundant coverage would occur if the UAV continues searching on the same curve, some offset perpendicular to the curve is required for the UAV, Fig 6. The offset required to avoid pseudo-redundant coverage is such that the UAV's sensing radius does not cover any part of the confidence area. Namely, it would be equal to the radius of the confidence circle at the UAV starting position left over by the time the UAV returned added to the UAV's sensing radius, Fig. 7:

$$d_{\perp\min} = (r_u - v_{t\max}l/v_u) + r_u. \tag{15}$$

Let us, now, suppose that the UAV gradually moves outward while making its way around the curve. The UAV must achieve the minimum offset, $d_{\perp\min}$, by the time it makes one round of the iso-probability curve. Thus, the offset required can be divided by the time it takes for the UAV to make one round of the curve to obtain the minimum perpendicular speed necessary to avoid pseudo-redundant coverage:

$$v_{\perp\min} = d_{\perp\min}/(l/v_u) = 2r_u v_u/l - v_{t\max} \tag{16}$$

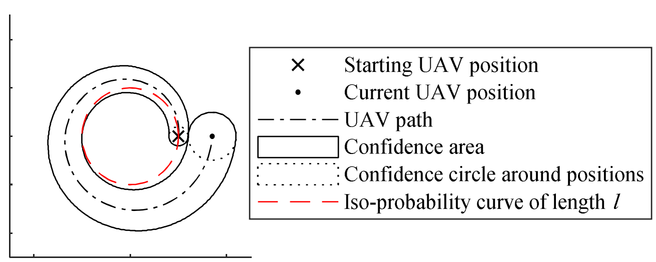


Fig. 6. The confidence area for a UAV searching on a (static) iso-probability curve of length $l$.

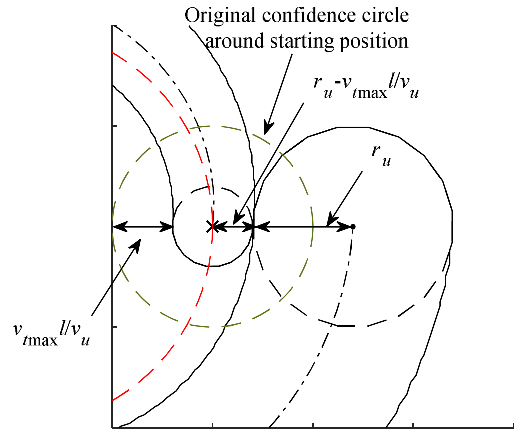


Fig. 7. A close-up look at the offset the UAV needs to achieve by the time it makes one full round of the (static) iso-probability curve.

*b) The Dynamic Iso-probability Curve Case*

When searching across a set of propagating iso-probability curves, the UAV must traverse these with the aim of intercepting the next curve after some amount of search effort is spent. Thus, the UAV would have a velocity perpendicular to the curve being searched at any instant. In order to avoid pseudo-redundant coverage, then, this velocity must be at least $v_{\perp\min}$ as is defined in (16).

When the UAV's heading to intercept the next iso-probability curve, on the next ray, is determined, the perpendicular component of the UAV's velocity is checked to ensure it is greater than $v_{\perp\min}$. If true, no action is taken. Otherwise, the UAV's heading is adjusted such that the perpendicular velocity is equal to $v_{\perp\min}$. The UAV, then, proceeds on the new heading until it intercepts its destination ray. Once achieved, search planning resumes as was described in Section IV.A.1.b.

*B. Multi-UAV Search Planning*

In single-UAV search planning described above, it was assumed that the UAV would search all the iso-probability curves. However, when there are multiple UAVs, the work needs to be divided between them to achieve a more efficient search. For example, let us consider that an $i^{\text{th}}$ UAV is designated to search from the $P_{i1}$% iso-probability curve to the $P_{i2}$% curve, where $P_{i1} < P_{i2}$. In this case, the percentile function would need to be modified such that the $i^{\text{th}}$ UAV would start searching on the $P_{i1}$% iso-probability curve and end on the $P_{i2}$% iso-probability curve:

$$p_i(E(t)) = C_i E_i(t)\,(P_{i2} - P_{i1}) + P_{i1}, \tag{17}$$

where $C_i$ and $E_i$ are the $i^{\text{th}}$ UAV's rate factor and cumulative effort function, respectively.

One way of allocating work is by optimally assigning UAVs to search non-intersecting subsets of the iso-probability curves in order to maximize the probability of target detection. Optimization can be carried out using methods such as gradient descent.

This is the author's version of the article that has been published at the Proc. Int. Conf. Unmanned Aircraft Syst., Atlanta, GA, USA, 2019, pp. 628-635.

Fig. 8 shows an example set of search trajectories for two UAVs, respectively, planned to cooperatively search for a mobile target. Both starting their motion at the target's LKP.

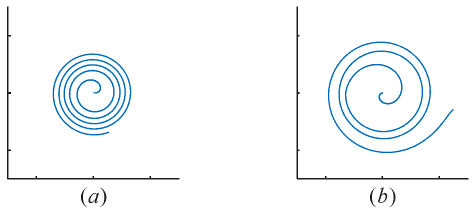


Fig. 8. Two UAV search paths: (*a*) UAV-1 and (*b*) UAV-2.

## V. Simulated UAV Experiments

Extensive simulated experiments were performed to validate the proposed UAV search-planning method for WiSAR. This section presents two illustrative examples as well as results from experiments comparing the proposed equal-effort search method to two alternative methods.

### A. An Illustrative WiSAR Example

In this example, it is assumed that a search is ordered to locate a lost person. Information provided suggests that the target is a novice hiker with a walking speed represented by a normal random variable with a mean of $\mu$ = 0.75 m/s and a standard deviation of $\sigma$ = 0.25 m/s [44]. The target is also assumed to be modeled using the motion model presented in [40] with a wandering parameter of $\sigma_\theta = \pi/3$ rad and a decisiveness parameter of $d_{\max}$ = 100 m. The pertinent terrain and obstacles information is also given, Fig. 9. In this figure, solid black regions denote impassable obstacles for the target. The actual target, in this example, was simulated to move with a walking speed of 0.72 m/s (unknown to the searchers).

A search was planned for two UAVs both with a maximum speed of 50 m/s and a ground-sensing radius of 25 m. Both UAVs were assumed to start their search at the LKP and move outward 3,600 s after the target was known to be there. The initial search was planned to run for 3,600 s such that the search would end 7,200 s after the target left its LKP. Optimal iso-probability curve assignments were determined to be 0-63% for UAV-1 and 63-100% for UAV-2, respectively.

In this example, the target was found at 6,705 s by UAV-1. Fig. 10 shows four snapshots of the search at 3,600 s, 4,635 s, 5,670 s, and 6,705 s, respectively. The red dot denotes the target position, while the UAVs are denoted by different colored circles (UAV-1 blue and UAV-2 red).

### B. Another Illustrative Example

In this example, the above search was planned for three UAVs, instead of two. Optimal iso-probability curve assignments were determined to be 0-47% for UAV-1, 47-77% for UAV-2, and 77-100% for UAV-3, respectively.

For the given scenario, the target was found at 5,605 s by UAV-2. Fig. 11 shows 4 snapshots of the search at 3,600 s, 4,270 s, 4,935 s, and 5,605 s, respectively. The red dot denotes the target position, while the UAVs are denoted by different colored circles (UAV-1 blue, UAV-2 red, and UAV-3 yellow).

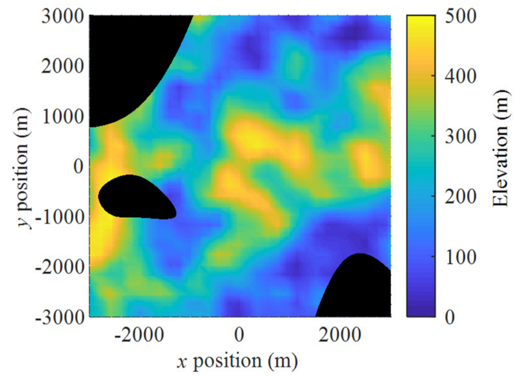


Fig. 9. The search area within which the illustrative example takes place.

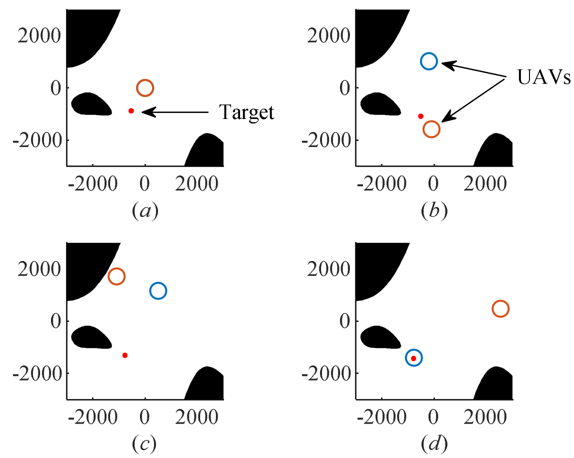


Fig. 10. Search at (*a*) 3,600 s, (*b*) 4,635 s, (*c*) 5,670 s, and (*d*) 6,705 s.

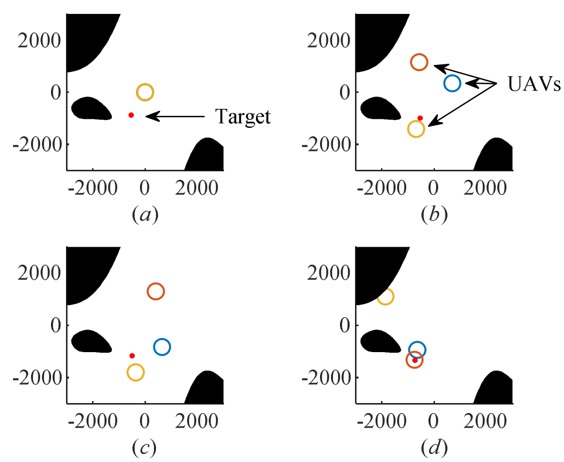


Fig. 11. Search at (*a*) 3,600 s, (*b*) 4,270 s, (*c*) 4,935 s, and (*d*) 5,605 s.

### C. Evaluating the Equal-Effort Search Method

In order to evaluate the performance of the proposed search planning method, it was compared to two alternative search algorithms: the constant-propagation method and the exhaustive method, respectively. In the former method, formulated in our laboratory, the (single) UAV moves radially outward at a constant rate. Unlike our method, this algorithm does not carry out any trajectory optimization as per the use of iso-probability curves. It is a simple geometric approach. In the latter method, based on the work presented in [31], the UAV progresses outward at a rate that ensures *complete* (100%) coverage of the search area as time progresses.

Fig. 12 below conceptually illustrates the radial position of the UAV as a function of time for all three methods.

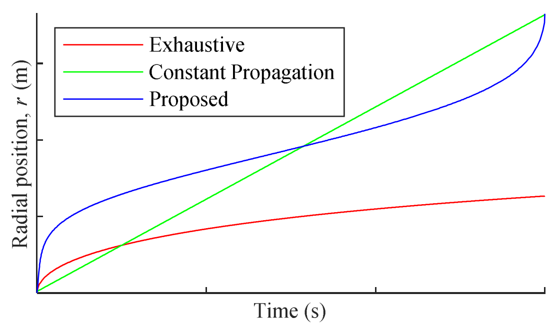


Fig. 12. Plot of UAV's radial position over time for the three search methods.

Extensive simulations were performed for various search scenario parameters. A representative set is given herein for four scenarios, simulated for the search of 1,000 distinct (random) targets. The number of targets detected was used as a measure of performance for a method, Table I. All searches started after 3,600s of target motion away from the LKP.

TABLE I. NUMBER OF TARGET DETECTIONS (OUT OF 1,000)

| ***Search length (s)*** | **1,600** | **3,200** | **4,800** | **6,400** |
|---|---|---|---|---|
| ***Proposed method*** | 310 | 504 | 577 | 593 |
| ***Constant-propagation*** | 203 | 333 | 388 | 414 |
| ***Exhaustive*** | 15 | 15 | 15 | 15 |
| ***ANOVA: F(2, 2,997)*** | 171 | 379 | 494 | 526 |
| ***p*** | < 0.0001 | < 0.0001 | < 0.0001 | < 0.0001 |

The above results validate that the proposed method outperforms the alternatives. One-way ANOVA tests showed that there was a statistical difference between the number of targets detected across all search lengths ($F(2, 2997) = 171.19$, $p<0.0001$). In particular, post-hoc pairwise Tukey's HSD criterion further validated that the difference between the proposed method and the constant-propagation method results was statistically significant regardless of the search length ($p < 0.0001$). As one would expect, however, the contrast between the proposed equal-effort and the constant-propagation methods diminishes as the search time becomes longer. This can be attributed to target-detection saturation. Namely, as the search time becomes longer, all targets are (nearly) exhaustively searched in both methods such that their performances become more similar.

One may note that the exhaustive search method performs poorly in the examples presented above since the target has ample time to move beyond the limits of where the method can maintain complete coverage. Thus, further experiments with earlier search start times and shorter search lengths were carried out, Table II. The results, as expected, showed that the exhaustive method can perform comparably to the proposed method when the start time is early enough that the UAV can completely cover an appreciable fraction of simulated targets.

TABLE II. NUMBER OF TARGET DETECTIONS (OUT OF 1,000)

| ***Start time (s)*** | **600** | | **900** | |
|---|---|---|---|---|
| ***Search length (s)*** | **150** | **700** | **150** | **700** |
| **Proposed method** | 915 | 969 | 792 | 950 |
| **Constant-propagation** | 559 | 955 | 295 | 812 |
| **Exhaustive** | 522 | 629 | 241 | 346 |

## VI. CONCLUSIONS

This paper presents a novel mobile-target search planning method for multi-UAV teams that utilizes target iso-probability curves. It is novel in that it proposes to have UAVs search across a range of iso-probability curves, expending equal effort on every curve while also avoiding pseudo-redundant coverage.

Several illustrative WiSAR experiments were presented to demonstrate how the method would perform under different scenarios. Further experiments comparing the proposed method to alternative UAV trajectory-planning algorithms, such as the constant-propagation and the exhaustive methods presented herein, were also performed. The results showed that the use of the proposed method results in a tangibly higher number of targets being detected.

While the proposed method has been primarily presented in the context of lost person search in WiSAR scenarios, it is applicable to any mobile-target search problem. Namely, the proposed method can be used for any (growing-area) search, wherein a target-location likelihood function can be estimated.

## REFERENCES

[1] R. Pierdicca, "Mapping Chimu's settlements for conservation purposes using UAV and close range photogrammetry. The virtual reconstruction of Palacio Tschudi, Chan Chan, Peru," *Digit. Appl. Archaeol. Cult. Herit.*, vol. 8, pp. 27–34, Mar. 2018.

[2] G. Zhang, B. Shang, Y. Chen, and H. Moyes, "SmartCaveDrone: 3D cave mapping using UAVs as robotic co-archaeologists," in *Proc. Int. Conf. Unmanned Aircraft Syst.*, Miami, FL, USA, 2017, pp. 1052–1057.

[3] M. Lazzari and D. Gioia, "UAV images and historical aerial-photos for geomorphological analysis and hillslope evolution of the Uggiano medieval archaeological site (Basilicata, southern Italy)," *Geomat. Nat. Hazards Risk*, vol. 8, no. 1, pp. 104–119, Jan. 2017.

[4] K. Zhao *et al.*, "Application research of image recognition technology based on CNN in image location of environmental monitoring UAV," *EURASIP J. Image Video Process.*, vol. 2018, no. 1, p. 150, Dec. 2018.

[5] F. S. Leira, T. A. Johansen, and T. I. Fossen, "A UAV ice tracking framework for autonomous sea ice management," in *Proc. Int. Conf. Unmanned Aircraft Syst.*, Miami, FL, USA, 2017, pp. 581–590.

[6] A. Tripolitsiotis, N. Prokas, S. Kyritsis, A. Dollas, I. Papaefstathiou, and P. Partsinevelos, "Dronesourcing: a modular, expandable multi-sensor UAV platform for combined, real-time environmental monitoring," *Int. J. Remote Sens.*, vol. 38, no. 8–10, pp. 2757–2770, May 2017.

[7] J. Navia, I. Mondragon, D. Patino, and J. Colorado, "Multispectral mapping in agriculture: Terrain mosaic using an autonomous quadcopter UAV," in *Proc. Int. Conf. Unmanned Aircraft Syst.*, Arlington, VA, USA, 2016, pp. 1351–1358.

[8] Jupriyanto, R. O. Bura, S. W. Apriyani, K. Ariwibawa, and E. Adharian, "UAV application for oil palm harvest prediction," *J. Phys. Conf. Ser.*, vol. 1130, p. 012001, Nov. 2018.

[9] J. Su *et al.*, "Wheat yellow rust monitoring by learning from multispectral UAV aerial imagery," *Comput. Electron. Agric.*, vol. 155, pp. 157–166, Dec. 2018.

[10] Lei Bin, Wang Ning, Xu Pengcheng, and Song Gangbing, "New Crack Detection Method for Bridge Inspection Using UAV Incorporating Image Processing," *J. Aerosp. Eng.*, vol. 31, no. 5, p. 04018058, Sep. 2018.

[11] D. Kang and Y.-J. Cha, "Autonomous UAVs for Structural Health Monitoring Using Deep Learning and an Ultrasonic Beacon System with Geo-Tagging," *Comput.-Aided Civ. Infrastruct. Eng.*, vol. 33, no. 10, pp. 885–902, 2018.

[12] C. A. Castiglioni, A. S. Rabuffetti, G. P. Chiarelli, G. Brambilla, and J. Georgi, "Unmanned aerial vehicle (UAV) application to the structural health assessment of large civil engineering structures," in *Proc. Int. Conf. Remote Sensing Geoinformation Env.*, Paphos, Cyprus, 2017, vol. 10444, p. 1044414.

[13] S. Rasmussen, K. Kalyanam, and D. Kingston, "Field experiment of a fully autonomous multiple UAV/UGS intruder detection and monitoring system," in *Proc. Int. Conf. Unmanned Aircraft Syst.*, Arlington, VA, USA, 2016, pp. 1293–1302.

[14] D. Perez, I. Maza, F. Caballero, D. Scarlatti, E. Casado, and A. Ollero, "A Ground Control Station for a Multi-UAV Surveillance System," *J. Intell. Robot. Syst.*, vol. 69, no. 1, pp. 119–130, Jan. 2013.

[15] A. Bakhtari, M. D. Naish, M. Eskandari, E. A. Croft, and B. Benhabib, "Active-vision-based multisensor surveillance - an implementation," *IEEE Trans. Syst. Man Cybern. Part C Appl. Rev.*, vol. 36, no. 5, pp. 668–680, Sep. 2006.

[16] J. Wang, Y. Tang, J. Kavalen, A. F. Abdelzaher, and S. P. Pandit, "Autonomous UAV Swarm: Behavior Generation and Simulation," in *Proc. Int. Conf. Unmanned Aircraft Syst.*, Dallas, TX, USA, 2018, pp. 1–8.

[17] F. J. Perez-Grau, R. Ragel, F. Caballero, A. Viguria, and A. Ollero, "Semi-autonomous teleoperation of UAVs in search and rescue scenarios," in *Proc. Int. Conf. Unmanned Aircraft Syst.*, Miami, FL, USA, 2017, pp. 1066–1074.

[18] N. M. Dinnbier, Y. Thueux, A. Savvaris, and A. Tsourdos, "Target detection using Gaussian mixture models and fourier transforms for UAV maritime search and rescue," in *Proc. Int. Conf. Unmanned Aircraft Syst.*, Miami, FL, USA, 2017, pp. 1418–1424.

[19] M. T. Agcayazi, E. Cawi, A. Jurgenson, P. Ghassemi, and G. Cook, "ResQuad: Toward a semi-autonomous wilderness search and rescue unmanned aerial system," in *Proc. Int. Conf. Unmanned Aircraft Syst.*, Arlington, VA, USA, 2016, pp. 898–904.

[20] T. Niedzielski, M. Jurecka, M. Stec, M. Wieczorek, and B. Miziński, "The nested k-means method: A new approach for detecting lost persons in aerial images acquired by unmanned aerial vehicles," *J. Field Robot.*, vol. 34, no. 8, pp. 1395–1406, Dec. 2017.

[21] T. Niedzielski and M. Jurecka, "Can Clouds Improve the Performance of Automated Human Detection in Aerial Images?," *Pure Appl. Geophys.*, vol. 175, no. 9, pp. 3343–3355, Sep. 2018.

[22] J. Sun, B. Li, Y. Jiang, and C. Wen, "A Camera-Based Target Detection and Positioning UAV System for Search and Rescue (SAR) Purposes," *Sensors*, vol. 16, no. 11, p. 1778, Oct. 2016.

[23] T. Niedzielski *et al.*, "A real-time field experiment on search and rescue operations assisted by unmanned aerial vehicles," *J. Field Robot.*, Mar. 2018.

[24] M. A. Goodrich *et al.*, "Supporting wilderness search and rescue using a camera-equipped mini UAV," *J. Field Robot.*, vol. 25, no. 1–2, pp. 89–110, Jan. 2008.

[25] T. Tomic *et al.*, "Toward a Fully Autonomous UAV: Research Platform for Indoor and Outdoor Urban Search and Rescue," *IEEE Robot. Autom. Mag.*, vol. 19, no. 3, pp. 46–56, Sep. 2012.

[26] M. A. Goodrich, J. L. Cooper, J. A. Adams, C. Humphrey, R. Zeeman, and B. G. Buss, "Using a Mini-UAV to Support Wilderness Search and Rescue: Practices for Human-Robot Teaming," in *Proc. IEEE Int. Workshop Safety Security Rescue Robot.*, Rome, Italy, 2007, pp. 1–6.

[27] T. Furukawa, F. Bourgault, B. Lavis, and H. F. Durrant-Whyte, "Recursive Bayesian search-and-tracking using coordinated uavs for lost targets," in *Proc. IEEE Int. Conf. Robot. Autom.*, Orlando, FL, USA, 2006, pp. 2521–2526.

[28] I.-K. Ha, Y.-Z. Cho, I.-K. Ha, and Y.-Z. Cho, "A Probabilistic Target Search Algorithm Based on Hierarchical Collaboration for Improving Rapidity of Drones," *Sensors*, vol. 18, no. 8, p. 2535, Aug. 2018.

[29] S. Perez-Carabaza, E. Besada-Portas, J. A. Lopez-Orozco, and J. M. de la Cruz, "Ant colony optimization for multi-UAV minimum time search in uncertain domains," *Appl. Soft Comput.*, vol. 62, pp. 789–806, Jan. 2018.

[30] L. Lin and M. A. Goodrich, "Hierarchical Heuristic Search Using a Gaussian Mixture Model for UAV Coverage Planning," *IEEE Trans. Cybern.*, vol. 44, no. 12, pp. 2532–2544, Dec. 2014.

[31] D. Brown and L. Sun, "Exhaustive mobile target search and non-intrusive reconnaissance using cooperative unmanned aerial vehicles," in *Proc. Int. Conf. Unmanned Aircraft Syst.*, Miami, FL, USA, 2017, pp. 1425–1431.

[32] Z. Tang and U. Ozguner, "On non-escape search for a moving target by multiple mobile sensor agents," in *Proc. American Control Conf.*, Minneapolis, MN, USA, 2006, pp. 3525–3530.

[33] J. Xie, L. R. G. Carrillo, and L. Jin, "An Integrated Traveling Salesman and Coverage Path Planning Problem for Unmanned Aircraft Systems," *IEEE Control Syst. Lett.*, vol. 3, no. 1, pp. 67–72, Jan. 2019.

[34] S. Hayat, E. Yanmaz, T. X. Brown, and C. Bettstetter, "Multi-objective UAV path planning for search and rescue," in *Proc. IEEE Int. Conf. Robot. Autom.*, Singapore, Singapore, 2017, pp. 5569–5574.

[35] F. Kunwar and B. Benhabib, "Rendezvous-Guidance Trajectory Planning for Robotic Dynamic Obstacle Avoidance and Interception," *IEEE Trans. Syst. Man Cybern. Part B Cybern.*, vol. 36, no. 6, pp. 1432–1441, Dec. 2006.

[36] M. Pelosi and M. S. Brown, "Improved search paths for camera-equipped UAVS in wilderness search and rescue," in *Proc. IEEE Symp. Series Comp. Intell.*, Honolulu, HI, USA, 2017, pp. 1–8.

[37] E. A. Croft, B. Benhabib, and R. G. Fenton, "Near-time optimal robot motion planning foe on-line applications," *J. Robot. Syst.*, vol. 12, no. 8, pp. 553–567, 1995.

[38] A. Macwan, J. Vilela, G. Nejat, and B. Benhabib, "A Multirobot Path-Planning Strategy for Autonomous Wilderness Search and Rescue," *IEEE Trans. Cybern.*, vol. 45, no. 9, pp. 1784–1797, Sep. 2015.

[39] A. Macwan, G. Nejat, and B. Benhabib, "Target-Motion Prediction for Robotic Search and Rescue in Wilderness Environments," *IEEE Trans. Syst. Man Cybern. Part B Cybern.*, vol. 41, no. 5, pp. 1287–1298, Oct. 2011.

[40] Z. Kashino, J. Y. Kim, G. Nejat, and B. Benhabib, "Spatiotemporal Adaptive Optimization of a Static-Sensor Network via a Non-Parametric Estimation of Target Location Likelihood," *IEEE Sens. J.*, vol. 17, no. 5, pp. 1479–1492, Mar. 2017.

[41] J. Vilela, Z. Kashino, R. Ly, G. Nejat, and B. Benhabib, "A Dynamic Approach to Sensor Network Deployment for Mobile-Target Detection in Unstructured, Expanding Search Areas," *IEEE Sens. J.*, vol. 16, no. 11, pp. 4405–4417, Jun. 2016.

[42] K. Woiceshyn, Z. Kashino, G. Nejat, and B. Benhabib, "Vehicle Routing for Resource Management in Time-Phased Deployment of Sensor Networks," *IEEE Trans. Autom. Sci. Eng.*, pp. 1–13, 2018.

[43] Z. Kashino, G. Nejat, and B. Benhabib, "A Hybrid Strategy for Target Search Using Static and Mobile Sensors," *IEEE Trans. Cybern.*, pp. 1–13, 2018.

[44] R. J. Koester, *Lost Person Behavior: A Search and Rescue Guide on Where to Look for Land, Air and Water*. Charlottesville, VA: dbS Productions, 2008.